INTERNATIONAL JOURNAL OF INTEGRATED ENGINEERING
ISSN: 2229-838X e-ISSN: 2600-7916

IJIE

Vol. 17 No. 4 (2025) 274-287
https://publisher.uthm.edu.my/ojs/index.php/ijie

Parametric Analysis of Blade Number Influence on the Aerodynamic Performance of a Savonius Rotor

Mohammed Ogab[1], Muhammad Faris Norazmi[2], Djamal Hissein Didane[3,4]*

[1] *Libyan Authority for Scientific Research, Tripoli, LIBYA*
[2] *EagleBurgmann (M) Sdn Bhd, Taman Perindustrian Tiong Nam, 40200 Shah Alam, Selangor, MALAYSIA*
[3] *Center for Energy and Industrial Environment Studies (CEIES), Faculty of Mechanical and Manufacturing Engineering, Universiti Tun Hussein Onn Malaysia 86400 Parit Raja, Batu Pahat, Johor, MALAYSIA*
[4] *National Institute of Sciences and Technology of Abeche, Abeche, CHAD*

*Corresponding Author: djamal@uthm.edu.my
DOI: https://doi.org/10.30880/ijie.2025.17.04.024

Article Info

Received: 12 March 2025
Accepted: 30 October 2025
Available online: 25 November 2025

Keywords

Savonius rotor, computational fluid dynamics (CFD), rotor design, performance analysis, VAWT, wind energy

Abstract

This study investigates the performance of two-blade and three-blade Savonius rotor wind turbines using computational techniques. The computational fluid dynamics (CFD) simulations are employed using Ansys Fluent as the flow solver while using the hybrid two-equation shear stress transport (SST) as the turbulence model. The performance investigation was based on torque, power and their conversion efficiencies at a ranging tip-speed ratio (TSR) between 0.2 to 1.2. The results of the simulation have been validated with existing work prior to presenting the present results in order to ensure their credibility and accuracy. The results have shown that both models with two-blade and three-blade have shown similar trends for all performance parameters tested. However, the analysis reveals substantial performance disparities between the two configurations. The three-blade design demonstrates superior characteristics, including higher torque values of 0.1077 Nm at TSR 0.8 and 0.434 for the power coefficient, Cp at the same TSR compared to the 2 blades, increased power generation, and improved power coefficients with 0.365 value at the highest TSR compared to the two-blade configuration. The examination of flow distributions has provided valuable insights into flow behavior, highlighting regions of acceleration, deceleration, and stagnation. This study contributes to the existing knowledge by illuminating the performance characteristics of two-blade and three-blade Savonius rotor turbines. The findings serve as a valuable resource for optimizing the design of efficient wind turbine systems, promoting the advancement of renewable energy generation.

1. Introduction

The utilization of energy has played a crucial role in human civilization, with advancements in technology and industries driving the need for increased energy generation, particularly electrical energy. However, the heavy reliance on fossil fuels and coal for electricity production has raised concerns about environmental pollution and depletion of natural resources [1]. Therefore, renewable energy is encouraged all over the world. Renewable energy sources such as wind, solar, hydropower and biomass are naturally occurring and abundant, providing a cleaner alternative with no pollution and carbon footprint [2]. As such, efforts are underway to shift reliance on fossil fuels and coal towards renewable energy sources, particularly wind and solar energies [3]. In the recent years, the global wind power sector demonstrated its prominence as a significant contributor to renewable energy, with an installed capacity surpassing 563GW. This impressive figure accounted for approximately 24% of the total renewable energy generation capacity worldwide. Among renewable energy sources, wind power emerged as the second most prevalent choice [4]. Wind energy is harvested through wind turbines by which these rotating devices will generate electricity by converting kinetic energy of rotating motion to electricity for residential, commercial, and industrial usage. High velocity wind will flow through the turbines creating drags and force causing the blades to rotate [5]. Two primary classifications of wind turbines for energy harvesting exist: horizontal axis wind turbines (HAWTs) and vertical axis wind turbines (VAWTs). The primary distinguishing characteristic between these two types lies in their respective rotating axes. Rotating axis that is parallel with the wind direction will be categorized as HAWT while if the rotating axis is perpendicular to the wind direction, it is called VAWT type. In general, studies have shown that HAWT type has better efficiency than VAWT type. HAWT is undoubtedly the superior option in terms of power production in steady wind conditions. When there is a consistent, strong wind stream, the HAWT can generate substantially more electricity [6].

One notable design of the VAWT category is the Savonius wind turbine. The fundamental structure of the simplest model of this turbine consists of a half-cylindrical component affixed to one side of a vertical shaft, forming a two-bladed configuration. This design harnesses the rotational power generated by the drag force, allowing the turbine to rotate at a speed exceeding that of the incoming wind. It is crucial for the tip speed ratio of the turbine to remain equal to or less than 1 for optimal performance [7]. The rotation of this turbine blades is driven by drag force. This force is generated as the wind interacts with the surfaces of the turbine blades, encompassing both the concave and convex sections. Compared to other drag-based machines, it exhibits a relatively low tip speed ratio. This characteristic poses limitations in terms of generating electricity, particularly when compared to devices that achieve higher tip speeds. In recent years, there have been advancements in the design of the Savonius turbine, leading to the development of new variants. These include configurations featuring spiral blades of shorter span mounted on a wide rotor hub, expanding the range of possibilities for this type of turbine [8].

Moreover, the Savonius wind turbine has a significant design defect in which a blade produces positive torque only during one half of the blade rotation, that is, when the blade is travelling in the same direction as the wind (advancing). When a blade moves against the wind (retreating), it provides negative torque, lowering the net torque supplied to the generator. As a result, a blade only produces power for about half of each rotation. It should come as no surprise that, while sturdy and simple to build, this design is not a genuine contender for significant power generation [9]. There are plenty of studies done to analyze the ability as well as the characteristics of the Savonius wind turbine. A comparative study has been done in 2012 where numerical study of detailed flow field is conducted on two Savonius Turbine designs: Conventional and Bach-type. Conventional Savonius-type rotor is simply the original design by S.J. Savonius while the Bach-type rotor is the modifies design wherein the model has a combination of straight and circular-arc in the shape of the blades. The result of the study shows that Bach-type rotor has a higher value of torque at the TSR 0.75. The result of the simulation also shows that the Bach-type rotor clearly has higher maximum power coefficient; 26.35%, compared to the conventional Savonius; 18.90% [10].

Furthermore, the performance of the Savonius rotor can be improved by simply changing or by slight alteration to the shape and dimension of the design [11]. In some studies researchers added some inner blades to the Savonius blades where the results show a significant improvement in the performance in terms of torque coefficient and power coefficient when inner blades are introduced. It was also concluded that the optimum inner blade angle is 120° due to its highest power coefficient value at 0.1885 [12]. The performance of the Savonius rotor can also be improved when it is placed in linear arrays. The closer the position between cluster of rotors linearly, the higher the efficiency [13]. In addition, another 2D numerical study performed using the same technique and the result shows that the overall torque coefficient percentage for the modified two turbine (cluster) is 20.18% and 17.04% which is clearly higher than a single turbine study [14]. Apart from that the number of blades can also vastly affect the Savonius rotor performance [15]. Sarath et al. [16] compared the performance of Savonius with 2, 3, and 4 blades as well as modified Bach-type rotor. The results show that the three blades performed better than the 2 and 4 blades while modified Bach-type has the highest performance overall due to the 41% overlap ratio. This idea could be supported more with another study by Wenehenubun et al. [17] where a comparative study was done on Savonius rotor with 2, 3, and 4 blades. The results happen to be similar where 3 blades have achieved highest performance with TSR value of 0.555 at the 7 m/s wind speed.

Similarly, Sudarma et al. [18] proves that increasing the blade number does enhance the torque and output power of wind turbines. By raising the pressure on the blade surface and focusing the wind flow at the blade tip, the winglet has an impact on performance [18]. On the other hand, swept and curved blades have also been recorded in a study to have an influence on HAWT performance. The study's result shows that converting the more efficient straight blades to sweeping and curved blades will significantly reduce efficiency when compared to the ante type [19]. Within the realm of VAWTs, such as the Savonius wind turbine, a slight efficiency disadvantage becomes apparent when compared to the HAWT type. This observation has been extensively validated through numerous studies. The maximum attainable efficiency for a Savonius rotor has been reported to reach up to 31%, whereas the HAWT type has demonstrated the capability to achieve efficiencies of up to 40% [20]. More research and development should be done for this particular wind turbine design in order for it to achieve higher efficiency and performance so that it can compete at the same level with HAWT type. This idea is one of the main reasons this study and investigation is being made to work.

Over the years, various methodologies were employed to assess the performance and efficiency of wind turbines, including experimental studies, numerical simulation, analytical investigations, and comparative studies. Notably, the CFD simulation serves as a valuable tool in the analysis of intricate problems involving fluid-fluid, fluid-solid, or fluid-gas interactions. Through the utilization of CFD, it becomes possible to predict the behavior of fluid systems by employing virtual models. The simulation process entails the incorporation of pertinent fluid and model attributes, ensuring the execution of simulations that yield high-quality data with a heightened level of accuracy. These data, in turn, plays a pivotal role in refining existing designs and, more significantly, evaluating the performance of Savonius wind turbines. Another way to enhance the performance of wind turbines is to use a counter rotating mechanism in the system wherein the wind energy wasted by the first turbine is utilized by the second turbine, in the case of a HAWT. A study by Zhiqiang et al. [21] shows that the effect of equal diameter counter rotating rotor can achieve higher power coefficient in large range of wind speed compared to conventional single HAWT rotor. The downstream wake flow's turbulence is intensified by the front Vice rotor's rotation, which improves fluid momentum and energy transmission while preventing blade surface separation. As a result, the main rotor power coefficient at a certain rotational speed is enhanced, and the lift drag ratio of the blade increases. In the case of vertical axis counter-rotating wind turbines, the rotors are put on top of each other while using a single shaft. This technique has shown an improvement of more than twofold [22].

Researchers at the University of Bristol have developed a blade design that can be adjusted to take advantage of the roll-up vortex created by the anhedral high sweeping angle from the leading edge to the tip. The adjustment can raise the coefficient of power for the blade design in this study to 137% [23]. As there is an increasing need and demand to utilize the renewable energy more and slowly reducing the environment harming operation of generating electricity, there is also a need for development of the electric generating wind turbine specifically Savonius rotor wind turbine. However, Savonius design suffers from lower efficiency compared to the other HAWT rotor. Therefore, this study aims to comprehensively evaluate the performance of the Savonius wind turbine while using different blade configurations, specifically focusing on two and three blades in order to improve its inherent low efficiency. The investigation employs the computational fluid dynamics (CFD) simulation as a valuable tool to obtain accurate and relevant solution. By conducting this study, a deeper understanding of the performance characteristics of the Savonius wind turbine will be attained, which will facilitate further advancements in VAWT rotor development. The more development done for this turbine, the more product can be designed and used especially at the residential area where the turbine needs to be in a simple design and cost effective unlike HAWT type rotor.

2. Theoretical Formulations

2.1 Turbulence Model Equation

The Reynolds-Averaged Navier-Stokes (RANS) equations are a set of mathematical equations used to simulate turbulent flow. These equations are derived by averaging the Navier-Stokes equations, which describe the motion of fluid, over a large number of flow realizations. The k-ω turbulence model is a specific type of RANS turbulence model that is commonly used for simulating wind turbine flows. It is based on two transport equations, one for the turbulent kinetic energy (k) and another for the specific dissipation rate (ω) and closed using a set of algebraic equations that relate the turbulent quantities to the mean flow properties. The SST (Shear Stress Transport) model is a specific variant of the k-ω turbulence model that is widely used in wind turbine simulations. It includes a blending function that smoothly transitions between the k-ω model in the viscous sublayer and the k-ε model in the free-stream which allows the SST model to accurately predict the near-wall behavior of the flow, which is critical for simulating the performance of a wind turbine.

The k-ω model is based on two transport equations, one for the turbulent kinetic energy (k) (Equation 1) and another for the specific dissipation rate (ω) (Equation 2). The kinetic energy (k) equation can be computed as below;

$$\frac{\partial(pk)}{\partial}+\frac{\partial(pku_i)}{\partial}=\frac{\partial}{\partial x_i}\left(\frac{\mu_t\partial k}{\partial x_j}\right)-\omega^2 \tag{1}$$

While the specific dissipation rate (ω) equation can be illustrated as follows;

$$\frac{\partial(p\omega)}{\partial t}+\frac{\partial(p\omega u_i)}{\partial x_i}=\frac{\partial}{\partial x_j}\left(\frac{\mu_t\partial\omega}{\partial x_j}\right)+\left(\frac{1}{\tau_\omega}\right)(\omega_t-\omega) \tag{2}$$

where t is time, μ_t is the turbulent viscosity, τ_ω is the specific dissipation rate relaxation time, ω_t is the turbulent production of specific dissipation rate. The two transport equations are closed using algebraic equations that relate the turbulent quantities to the mean flow properties. The SST model uses a blending function that smoothly transitions between the k-ω model in the viscous sublayer and the k-ε model in the free-stream.

2.2 Performance Parameters

The Performance parameters are crucial for studying the performance of wind turbines. They provide a way to quantify the efficiency and effectiveness of a turbine's design and operation. The most commonly used performance parameters for wind turbines include torque, power, tip speed ratio, power coefficient, and torque coefficient. Torque (Equation 3) is a measure of the turning force on the turbine, while power (Equation 4) is a measure of the rate at which energy is generated. The tip speed ratio (Equation 5) is the ratio of the speed of the tip of the turbine blades to the wind speed, and it plays a role in the turbine's aerodynamics. The power coefficient (Equation 6) is a measure of how much of the available wind power is being converted into usable electricity by the turbine. The torque coefficient (Equation 7) is a measure of how much of the available wind torque is being converted into usable electricity. These parameters are used to evaluate the turbine's performance, optimize the design and operation, and compare the performance of different turbine designs.

$$\tau = \frac{P}{\omega}\ (N.m) \tag{3}$$

$$P = \frac{1}{2}\rho A u^3\ (W) \tag{4}$$

$$\gamma = \frac{\omega R}{U}\ (-) \tag{5}$$

$$C_p = \frac{\tau}{\frac{1}{2}\rho A u^3}\ (-) \tag{6}$$

$$C_t = \frac{\tau}{\frac{1}{2}\rho A u^3}\ (-) \tag{7}$$

3. Methodology

3.1 Savonius Wind Turbine 3D Model

As illustrated in Fig. 1, the 3D model with 2-blade Savonius wind turbine for this study is presented. The structure is modelled based on the geometrical features shown in Table 1 where the diameter of the rotor is 150 cm and the gap between the root of blade is 0.15d which is equal to 11.25 mm. The height of the rotor is 100 cm, as shown in Table 1. Fig. 2 shows the simulation domain of the simulation. It refers to the region of space that is being simulated. It is the region of space where the governing equations of fluid flow and heat transfer are solved. The simulation domain is defined by the geometry of the system or component being analyzed, and it includes all the regions of the model that are relevant to the problem being studied.

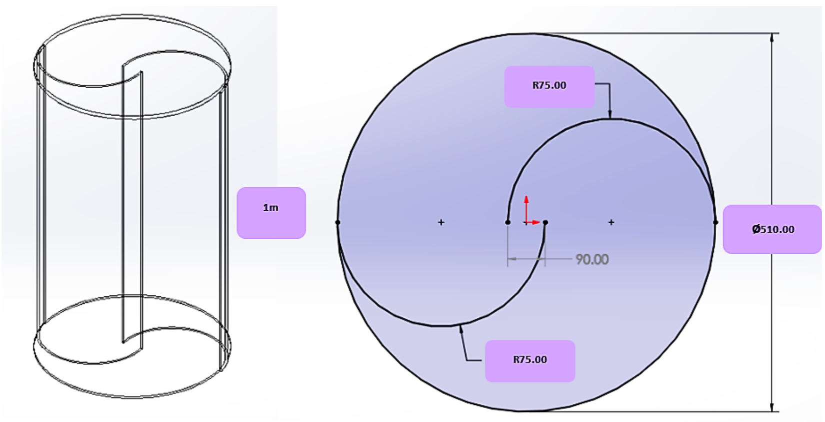

Fig. 1 *Dimension for 3D Savonius with 2 blade model*

Table 1 *Geometrical parameters of the simulation model*

Parameter	Details
Rotor type	Conventional Savonius
Rotor diameter, D	150 mm
Blade diameter, d	7.5 cm
End plate diameter, Do	16.5 cm
Blades thickness, t	1 mm
Overlap ratio, e	0.15d
Gap ratio, g	0
Rotor height, H	100 cm

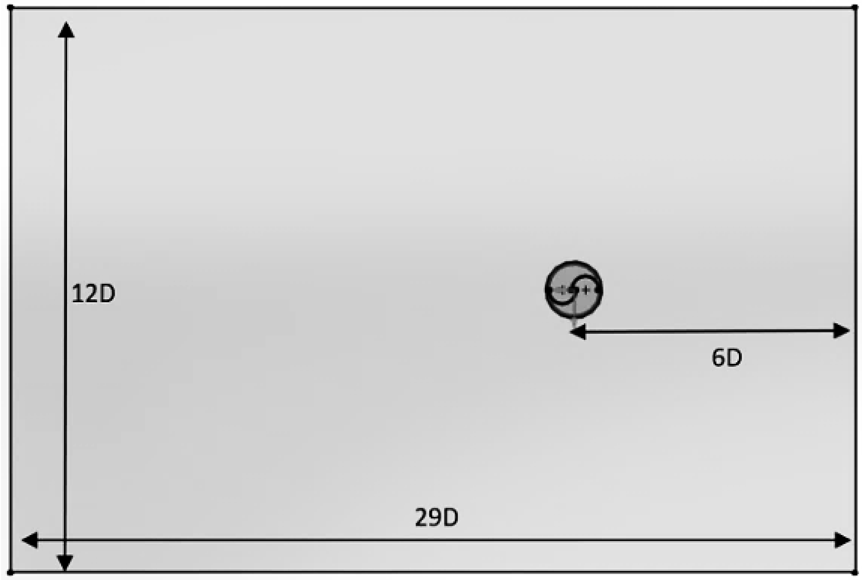

Fig. 2 *Computational simulation domain*

3.2 Boundary Conditions and Spatial Domain Discretization

Computational modelling requires boundary conditions to define the physical system's constraints. CFD simulation outcomes depend on precisely specifying boundary conditions for each component's geometry during pre-processing. Improper boundary conditions might cause simulation errors. Fluid dynamics simulations have many variables and boundaries. In this particular study, a steady velocity distribution was applied at the inlet in the direction of the x-axis. An atmospheric pressure boundary condition was applied at the outlet. Meanwhile a stationary wall with no slip shear condition and a standard roughness model were used at the side walls as well as rotor blades. Other than that, this study has also incorporated two interfaces, one at the rotating region and the other at the static domain region. The simulation domain can be divided into different regions, each with its own set of boundary conditions and material properties, as shown in Fig. 2. For example, a fluid flow simulation may have different regions for inlet, outlet, walls, and internal regions. Each region will have its own set of boundary conditions such as velocity, pressure, temperature, etc. and material properties such as density, viscosity, thermal conductivity, etc. The dimension and positioning of domain for this study are adopted from the previous literature also by Kumar et al. [24].

Moreover, meshing is among the most critical processes in completing an accurate simulation. The meshes are composed of elements that contain nodes that describe the geometry's form. Therefore, as shown in Fig. 3, the adaptive parameters from the mesh dimensioning feature are used to obtain more uniform mesh cells around the domain, allowing for an evenly distributed composition of the mesh cells around the airfoil body, as the validity and reliability of the flow solution are heavily dependent on the effectiveness of the mesh cells generated in this process. Furthermore, in order to obtain accurate results, the grid-independent test was performed. The mesh independence is obtained by successfully completing several levels of re-meshing refinements. In this study, four levels of element sizing were used to gradually optimize the mesh, particularly around the air foil, which is the most important component of this study.

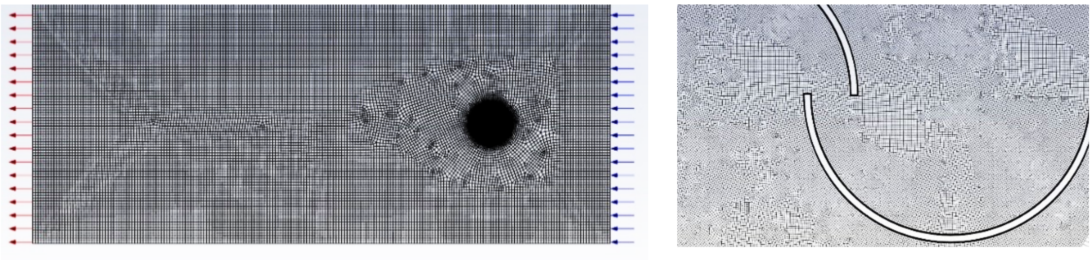

Fig. 3 *Mesh generated on the two-blade model (a) Meshing of the domain; (b) Close up view of mesh near the rotating interface*

4. Results and Discussion

4.1 Model Validation

In order to ensure the credibility of the simulation results, researchers must ensure compatibility between the simulation model and the selected literature for comparison. This ensures the reliability and accuracy of the obtained results based on the percentage difference analysis. In this study, specific settings and parameters were derived from a previous study [24] and applied in the current simulation. By maintaining consistency in these settings, researchers aim to achieve simulation results that closely align with the expected outcome, facilitating meaningful analysis, discussion, and conclusion. Similar trends or results would indicate the correctness of the simulation and the validity and reliability of the obtained results. The comparison was performed in the form of torque coefficient, C_t versus TSR, as shown in Fig. 4. Based on the comparison results, it is evident that the average percentage difference for the 2-blade configuration is 7.64%. This outcome indicates the validity of the simulation and its model. Consequently, all the data obtained can be considered suitable for discussion and drawing conclusions.

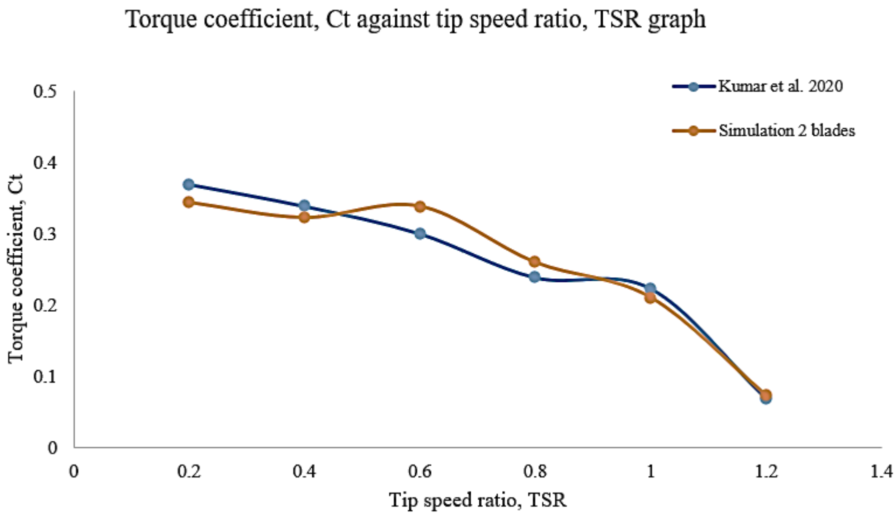

Fig. 4 *Validation graph as compared to the previous study*

4.2 Torque Performance Analysis

Based on the torque data acquired from the simulations, it can be deduced that the torque values for both the 2-blade and 3-blade configurations exhibit a decreasing trend as the tip speed ratio (TSR) increases, as shown in Fig. 5. This inverse relationship between torque and TSR is evident in the plotted data presented in Fig. 5. The observed trend confirms the claim that torque is inversely proportional to TSR, as higher TSR values correspond to lower torque values. In the context of the 2-blade configuration, the torque values demonstrate a gradual decline with increasing TSR. Particularly, at lower TSR values, such as 0.2 and 0.4, the torque values exhibit relatively high magnitudes of 0.15152703 Nm and 0.14214396 Nm, respectively. However, as the TSR exceeds 0.4, a significant decline in the torque values becomes evident. This decline indicates a decrease in the efficiency of converting wind energy into rotational mechanical energy. At a TSR of 1.2, the torque values reach their minimum point, measuring 0.03263086 Nm. This observation suggests a diminished power generation efficiency for the 2-blade configuration at higher TSRs.

In contrast, the 3 blade Savonius turbine exhibits a distinct behavior. Initially, as the TSR increases from 0.2 to 0.4, the torque values show a progressive rise, reaching a peak at a torque of 0.22105050 Nm. This signifies an enhanced energy conversion efficiency compared to the 2-blade configuration within this TSR range. However, as the TSR further increases, the torque values exhibit a gradual decline, although at a slower rate compared to the 2-blade configuration. Across all TSR values, the torque values for the 3-blade configuration consistently exceed those of the 2-blade configuration. Remarkably, at a TSR of 1.2, the torque value for the 3 blade configuration measures 0.13393838 Nm, indicating its superior power generation capabilities at higher TSRs relative to the 2-blade counterpart. Moreover, the observed trend aligns with the reference simulation, as it also demonstrates a decreasing pattern. This agreement between the obtained results and the reference simulation further supports the validity and reliability of the findings.

These findings emphasize the impact of blade count on Savonius wind turbine performance. When compared to the 2-blade arrangement, the 3-blade configuration has greater torque values, showing superior energy conversion efficiency throughout a wide range of TSRs. The variance in torque values with rising TSR values shows that the two layouts have different aerodynamic characteristics and flow dynamics. This analysis offers useful information for the design and optimization of Savonius wind turbines. The data backs up the idea that increasing the number of blades can improve power generation efficiency, especially at higher TSRs. Further research could look at the underlying flow phenomena and aerodynamic principles that are causing the observed trends, which could aid in the construction of more efficient and effective Savonius wind turbine designs.

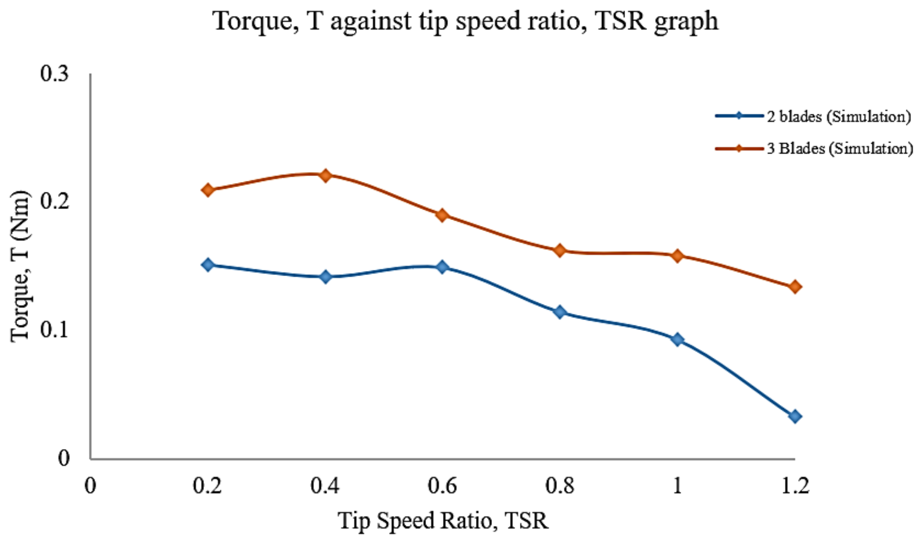

Fig. 5 *Torque output against tip speed ratio*

4.3 Torque Coefficient Performance Analysis

The torque coefficient serves as a dimensionless measure that encapsulates the efficacy of a wind turbine in the conversion of wind's kinetic energy into rotational mechanical energy. This coefficient is determined by taking the ratio of the torque produced by the wind rotor to the product of the dynamic pressure of the incoming wind and the swept area of the rotor. As a pivotal parameter, the torque coefficient is extensively employed to evaluate wind turbines' performance and enable efficiency comparisons under varying operational circumstances. The graph depicting the relationship between torque coefficient and TSR unveils distinct patterns and performance characteristics for the 2-blade and 3-blade configurations of Savonius wind turbines, as shown in Fig. 6. In the case of the 2-blade configuration, the torque coefficient exhibits a gradual decline with increasing TSR. Notably, at lower TSR values such as 0.2 and 0.4, the torque coefficient demonstrates relatively higher values of 0.3436 and 0.3223, respectively. However, as the TSR surpasses 0.4, a significant reduction in the torque coefficient becomes evident. This decline signifies a diminishing efficiency in converting wind energy into rotational mechanical energy. The minimum torque coefficient value of 0.0740 is observed at a TSR of 1.2, indicating a decreased power generation efficiency for this particular configuration at higher TSRs.

Conversely, the 3 blade Savonius turbine displays a distinct pattern. The torque coefficient exhibits an initial increase as the TSR elevates from 0.2 to 0.4, ending in a peak value of 0.5012. This signifies an enhanced energy conversion efficiency compared to the 2-blade configuration at these TSR values. However, as the TSR continues to rise, the torque coefficient gradually diminishes, albeit at a slower rate compared to the 2-blade configuration. Throughout the entire range of TSR values, the torque coefficient for the 3-blade configuration consistently remains relatively higher than that of its 2 blade counterparts, with a minimum value of 0.3037 recorded at TSR 1.2. These findings suggest that the 3 blade Savonius turbine sustains superior power generation capabilities, particularly at higher TSRs, in comparison to the 2-blade configuration.

The findings underscore the significant impact of the number of blades on the performance of Savonius wind turbines. Specifically, the 3-blade configuration demonstrates higher torque coefficients, indicative of superior energy conversion efficiency across a different range of TSRs compared to the 2-blade configuration. The observed variations in torque coefficients as TSR values increase suggest disparities in aerodynamic characteristics and flow dynamics between the two configurations. These insights hold considerable value for the design and optimization of Savonius wind turbines. The results support the notion that increasing the number of blades can effectively enhance power generation efficiency, particularly at higher TSRs. Future investigations could reach deeper into the underlying flow phenomena and aerodynamic mechanisms responsible for the identified trends. Such efforts would contribute to the development of more efficient and impactful Savonius wind turbine designs, propelling the advancement of sustainable energy technologies.

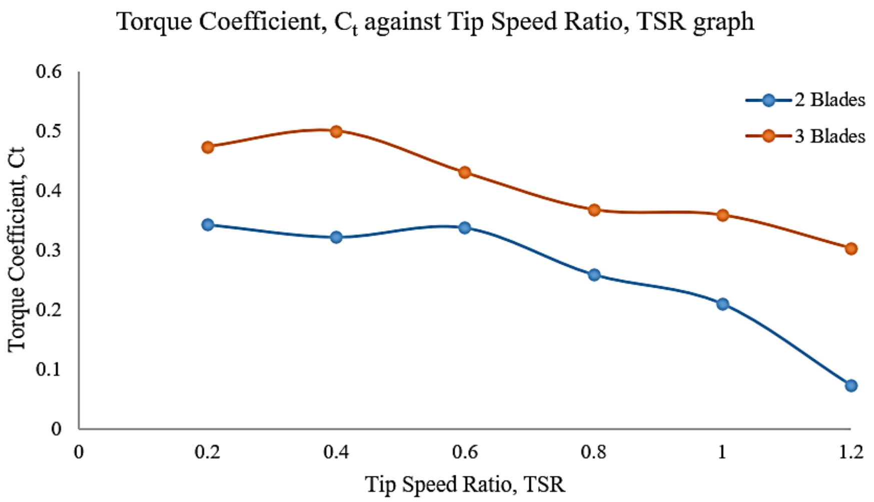

Fig. 6 *Torque coefficient against tip speed ratio*

4.4 Power Performance Analysis

Power in wind rotor simulations represents the rate at which mechanical energy is generated by a wind turbine, achieved through the conversion of wind kinetic energy into rotational motion. This fundamental parameter serves to quantify the energy output of the wind turbine and is commonly expressed in watts (W) or kilowatts (kW). The power generated is influenced by various factors such as wind speed, rotor size, and turbine efficiency. The power output of the 2-blade configuration progressively increases as the TSR ascends from 0.2 to 1.0, reaching a peak value of 9.9114 W. However, at a TSR of 1.2, the power output drops drastically to 4.1768 W, as shown in Fig. 8 (sub-topic 4.5). This indicates a reduction in power generation efficiency at higher TSRs, implying that the turbine is not performing optimally under these conditions. The 3-blade arrangement, on the other hand, follows a different pattern. As the TSR climbs from 0.2 to 1.2, the power output continuously increases, reaching a maximum of 17.1441 W. This implies that the 3-blade turbine layout can generate more power across the whole range of TSRs than the 2-blade configuration. Clearer depiction of the trend can be envisioned in the Power, P against tip speed ratio, TSR graph shown in Fig. 7.

These findings highlight the impact of the number of blades on Savonius wind turbine power generation capabilities. The 3-blade configuration outperforms the 2-blade configuration in terms of power output, especially at higher TSRs. This demonstrates the potential advantages of increasing the number of blades in enhancing the efficiency and overall power production of Savonius wind turbines. Further investigation and analysis of the underlying aerodynamic and flow characteristics can provide useful insights for optimizing the design and operational parameters of Savonius wind turbines, resulting in improved power production efficiency and performance.

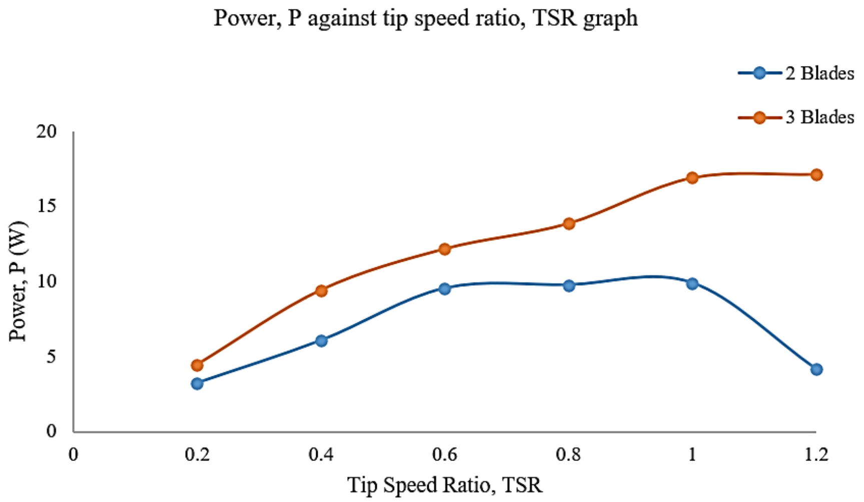

Fig. 7 *Power output against tip speed ratio*

4.5 Power Coefficient Performance Analysis

The power coefficient assumes a dimensionless nature and serves as a metric to evaluate the efficiency of a wind turbine by extracting energy from the wind. It is defined as the ratio between the actual power generated by the turbine and the maximum possible power extractable from the wind at a given wind speed and rotor area. A higher power coefficient signifies a more efficient conversion of wind energy into mechanical power, indicating enhanced performance. Conversely, a lower power coefficient implies reduced efficiency and diminished energy extraction capabilities. Analyzing power and power coefficient is of utmost importance in assessing performance, optimizing design, and predicting the energy output of wind turbines. These parameters enable researchers and engineers to evaluate the efficiency of various turbine configurations, compare performance across designs, and make well-informed decisions for maximizing power generation from wind resources.

Based on Fig. 8, in the case of the 2-blade configuration, the power coefficient rises from TSR 0.2 to 1.0, that ends at 0.2107. However, at TSR 1.2, there is a substantial decrease, resulting in a decreased power coefficient of 0.0888. This reduction indicates a decline in the efficiency of wind energy extraction at higher TSRs for this particular configuration. The 3-blade arrangement, on the other hand, behaves differently. As the TSR grows from 0.2 to 1.2, the power coefficient continuously increases, reaching a maximum value of 0.3645. This suggests a more efficient conversion of wind energy into mechanical power than the 2-blade arrangement, particularly at higher TSRs. When comparing the power coefficients of the two designs, it is evident that the 3 blade Savonius turbine consistently outperforms the 2-blade configuration across the entire range of TSRs. The higher power coefficients achieved by the 3-blade arrangement indicate its superior capability to harness wind energy and convert it into mechanical power more effectively. These findings emphasize the significance of blade arrangement in optimizing the power coefficients and overall performance of Savonius wind turbines. The utilization of a greater number of blades, as exemplified by the 3-blade configuration, contributes to enhanced efficiency in power extraction and improved energy conversion capabilities.

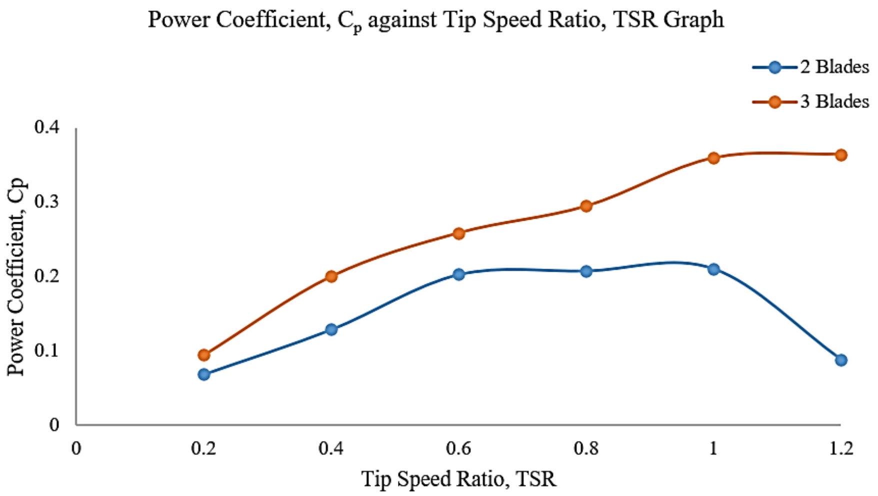

Fig. 8 *Power coefficient against tip speed ratio*

Conducting additional investigations into the aerodynamic characteristics and flow dynamics of the 3 blade Savonius configuration can yield valuable insights into the underlying mechanisms that contribute to its superior performance. These insights have the potential to significantly impact the design and operational parameters of Savonius wind turbines, facilitating the development of more efficient and effective turbine configurations. By optimizing these configurations based on a comprehensive understanding of the aerodynamic phenomena involved, the power generation potential from wind resources can be maximized.

4.6 Discussion

Upon analyzing the torque coefficient data from the simulations of both the 2 blade and 3 blade Savonius turbines, a clear observation emerges: the 3-blade configuration consistently demonstrates higher torque coefficients across the entire range of TSR values in comparison to the 2-blade configuration. This finding suggests that the 3-blade design possesses superior efficacy in extracting rotational mechanical energy from the wind. Moreover, as the TSR increases, the torque coefficients of the 3-blade configuration remain notably higher than those of the 2-blade configuration. This supports the notion that the 3-blade arrangement maintains enhanced power generation capabilities, particularly at higher TSR values. Upon examining the torque data, a similar pattern emerges as in the previous analysis. As the TSR increases, the torque values decrease for both the 2 blade and 3 blade configurations. However, it is noteworthy that the torque values of the 3-blade configuration consistently surpass those of the 2-blade configuration across all TSR values. This reaffirms the superior power generation capabilities of the 3-blade design, especially at higher TSRs. Examining the power generation aspect makes it apparent that the power output rises with an increase in TSR for both the 2 blade and 3 blade configurations.

Nevertheless, it is worth noting that the power values of the 3-blade configuration consistently exceed those of the 2-blade configuration across all TSR values. This provides additional evidence to substantiate the notion that the 3-blade design excels in converting wind energy into mechanical power. Upon analysis of the power coefficient data, it becomes apparent that the 3-blade configuration consistently attains superior power coefficients when compared to the 2-blade configuration across the entire range of TSRs. This observation suggests that the 3-blade design possesses enhanced capabilities for harnessing wind energy and converting it into mechanical power. Notably, the power coefficients for both configurations generally exhibit an upward trend with increasing TSR, signifying an improved efficiency in extracting energy at higher TSR values.

Collectively, the analyses conducted on the torque, power generation, and power coefficient data underscore the favorable attributes of the 3-blade configuration when compared to its 2-blade configuration. The results strongly indicate that increasing the number of blades in the Savonius turbine design confers notable advantages in terms of energy conversion efficiency and power generation capabilities, particularly at higher TSRs. These significant findings hold valuable implications for the optimization and design of Savonius wind turbines, as they pave the way for the development of more efficient and effective turbine configurations aimed at maximizing power generation from wind resources.

4.7 Visualization and Analysis of Flow Patterns

Flow pattern visualization and analysis are vital for understanding fluid dynamics in engineering applications. CFD simulations enable the visualization and analysis of flow patterns, offering insights into system performance. In this subtopic, the qualitative analysis of flow patterns using 2D CFD simulations has been explored. By visualizing pressure and velocity contours, as well as streamlines, researchers can gain valuable information about fluid behavior and its impact on system performance. These visual representations aid in optimizing system design and operation by revealing the underlying mechanisms of fluid flow. The velocity contours obtained offer significant insights into the flow behavior within the air flow domain. Analyzing the velocity distribution across the contour offers a comprehensive examination of spatial variations in flow velocities, facilitating the identification of regions characterized by flow acceleration, deceleration, or stagnation. Consequently, a more profound comprehension of the flow characteristics around the Savonius rotor blades can be attained.

Taking one example of a velocity contour obtained from the 3-blade simulation of TSR of 1.2 and angular speed, ω of 128 Rad/s as depicted in Fig. 9, the velocity contour obtained provides valuable insights into the flow behavior within the analyzed system. The contour unveils visible patterns and fluctuations in flow velocities across the entirety of the domain. Notably, the tip of the blades labelled (a) in Fig. 10 within the rotating core exhibits areas characterized by increased velocities, indicative of intensified flow or localized acceleration with maximum velocity of 11.7 m/s. These regions are likely a consequence of the high velocity flow established by the velocity inlet. Conversely, regions denoted as (b) at the back of the advancing blade display low velocities or stagnation, suggesting impeded flow or hindrance caused by counter torque. The contour also reveals the presence of flow gradients and streamlines, illustrating the directional flow pathways and fluid movement within the system. Notably, areas of flow separation and recirculation are observed, indicating the occurrence of vortex shedding and boundary layer separation. These flow phenomena can be attributed to the interaction between the fluid and the blade surfaces, as well as the geometric features of the 3-blade Savonius rotor. Additionally, the contour illustrates the interaction between the fluid and the rotor housing, leading to the formation of flow disturbances and wake regions behind the blades.

Subsequently, the velocity contour highlights the presence of notable features or irregularities, demanding additional study and analysis. Such features can include areas of flow stagnation, localized turbulence, or the formation of secondary vortices. These irregularities in the flow patterns deviate from the expected behavior and may stem from phenomena like flow separation, adverse pressure gradients, or fluid instabilities. Understanding and characterizing these deviations are crucial as they can have implications for system efficiency, performance, or even safety considerations. Thus, further investigation is required to elucidate the underlying causes and assess their potential impact on the overall performance and operation of the system studied.

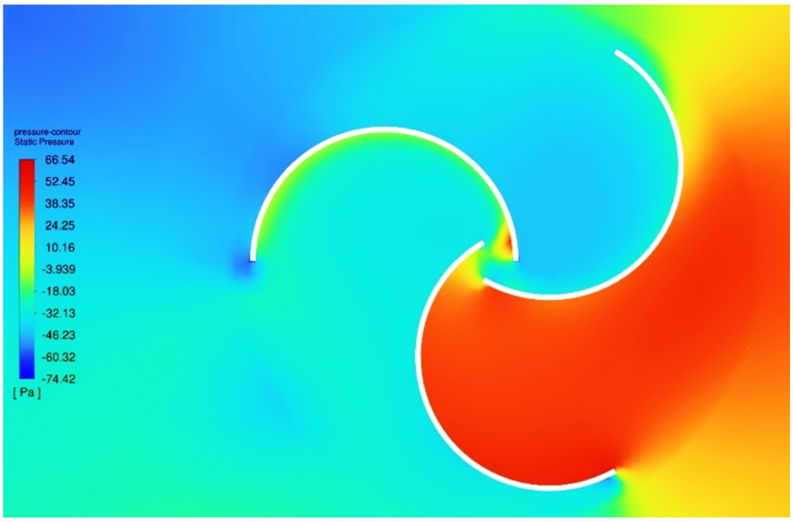

Fig. 9 *Pressure contours for 3 blade model*

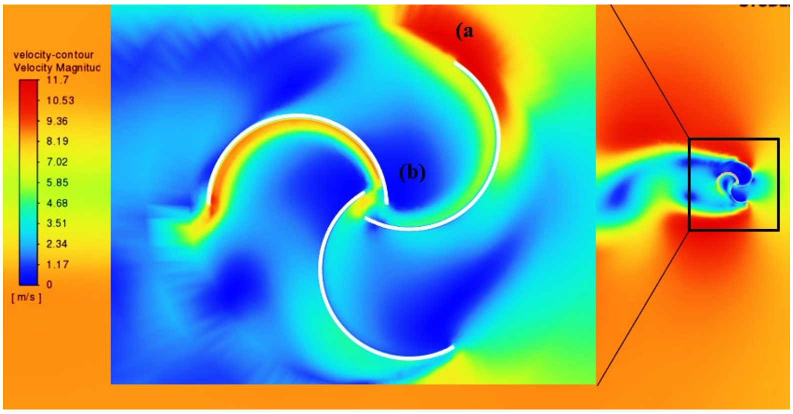

Fig. 10 *Velocity contours for 3 blade model*

Moreover, the pressure contour obtained in Fig. 9 provides valuable insights into the behavior and characteristics of the fluid flow around the 3-blade Savonius rotor. Analyzing the pressure distribution across the contour, we can observe variations in pressure levels, identifying areas of high and low pressure. The contour reveals the presence of alternating regions of high and low pressure, signifying the existence of pressure gradients and spatial variations in pressure magnitude and direction. These pressure gradients can indicate areas of pressure rise or drop, highlighting the occurrence of flow separation and pressure differentials across the blades. Notably, the pressure contour exhibits distinct pressure anomalies in the area of the blade edges, with localized pressure drops and higher-pressure zones near the trailing edges that gives a static pressure reading of maximum 66.54 Pa. These anomalies could be attributed to the formation of vortex shedding and flow recirculation, resulting in fluctuating pressure patterns along the blade surfaces. These pressure anomalies may have implications for the overall aerodynamic performance and efficiency of the Savonius rotor, affecting the lift and drag forces experienced by the blades. Furthermore, the pressure contour enables us to assess the effects of pressure distribution on the surrounding surfaces and objects, influencing the structural integrity of the rotor and its interaction with the surrounding flow field.

Furthermore, the streamlines serve as visual indicators of the flow's trajectory, revealing essential features and phenomena within the airflow domain surrounding the Savonius rotor, as in Fig. 11. Remarkably, distinct regions of vorticity and swirling motion become evident, underscoring the prevalence of rotational flow patterns. The emergence of these flow patterns can be attributed to various factors, including the geometric configurations of the rotor blades and the complex interaction between the fluid and solid surfaces. This visualization facilitates the identification of any visible irregularities or deviations within the flow. Noteworthy separation zones and recirculation regions become apparent, offering valuable insights into the complex interaction between flow separation, vortex shedding, and boundary layer behavior. These deviations from anticipated flow behavior offer crucial cues for understanding the efficiency and performance of the Savonius rotor, as well as its potential for power generation. They prompt the need for meticulous investigation and thoughtful consideration during the analysis process to optimize the design and maximize the system's capabilities.

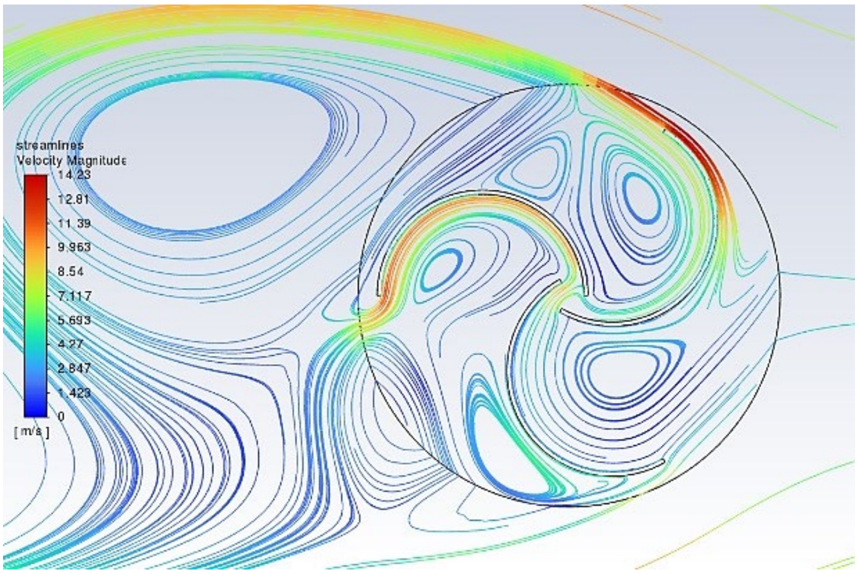

Fig. 11 *Velocity streamlines for 3 blade model*

5. Conclusion

This study presents a comprehensive analysis of two- and three-blade Savonius wind rotor turbines using advanced CFD methods. The following conclusions can be drawn from this study:

i. The torque values exhibited an inverse relationship with tip speed ratio (TSR) for both the 2-blade and 3-blade configurations.
ii. The 3-blade configuration consistently demonstrated higher torque values compared to the 2-blade configuration across a wide range of TSRs.
iii. The power coefficient also showed an inverse relationship with TSR for both configurations.
iv. The 3-blade configuration consistently displayed higher power coefficients compared to the 2-blade configuration across all TSR values.
v. The power output for the 3-blade configuration consistently exceeded that of the 2-blade configuration.
vi. The maximum power output recorded for the 3-blade configuration was 17.14 W, while the 2-blade configuration reached a maximum of 9.91 W.
vii. The flow visualisations provided insights into flow behavior, indicating regions of acceleration, deceleration, and stagnation.

Future research should prioritize optimizing blade geometry for Savonius wind turbines by exploring variables such as curvature, aspect ratio, and twist angle to improve aerodynamic efficiency and power output. Additionally, advancing numerical simulation methods by exploring alternative turbulence models, meshing techniques, and numerical schemes is essential. These improvements can increase simulation accuracy and reliability, though current efforts are limited by computational constraints.

Acknowledgement

Communication of this research is made possible through monetary assistance by Universiti Tun Hussein Onn Malaysia and the UTHM Publisher's Office via Publication Fund E15216.

Conflict of Interest

Authors declare that there is no conflict of interest regarding the publication of the paper.

Author Contribution

The authors confirm contribution to the paper as follows: ***study conception and design:*** *Muhammad Faris Norazmi;* ***data collection:*** *Mohammed Ogab;* ***analysis and interpretation of results:*** *Muhammad Faris Norazmi, Mohammed Ogab;* ***draft manuscript preparation:*** *Djamal Hissein Didane. All authors reviewed the results and approved the final version of the manuscript.*

References

[1] Didane, D. H. (2018). Wind and solar assessment in the sahelian zone of chad. International Journal of Integrated Engineering, 10(8). https://doi.org/10.30880/ijie.2018.10.08.026

[2] Ali R., Daut, I., & Taib, S. (2012) A review on existing and future energy sources for electrical power generation in Malaysia, *Renewable and Sustainable Energy Reviews*, *16(6)*, 4047-4055. https://doi.org/10.1016/j.rser.2012.03.003

[3] Alharthi M., Hanif, I., & Alamoudi, H. (2022) Impact of environmental pollution on human health and financial status of households in MENA countries: Future of using renewable energy to eliminate the environmental pollution, *Renewable Energy*, *190*, 338-346. https://doi.org/10.1016/j.renene.2022.03.118

[4] EIA. (2021, January 30). U.S. Energy Information Administration, Country analysis executive summary: Malaysia. *Independent Statistic & Analysis*. https://www.eia.gov/international/analysis/country/MYS

[5] Mondal M., Didane, D. H., Ali, A. H. I., & Manshoor, B. (2022) Technical assessment of wind energy potentials in Bangladesh, *Journal of Advanced Research in Fluid Mechanics and Thermal Sciences*, *96(2)*, 10-21. https://doi.org/10.37934/arfmts.96.2.1021

[6] Didane D. H., Wahab, A. A., Shamsudin, S. S., Rosly, N., Zulkafli, M. F., & Mohd, S. (2017) Assessment of wind energy potential in the Capital City of Chad, N'Djamena. In *AIP Conference Proceedings*, *831(1)*, 020049. AIP Publishing LLC. https://doi.org/10.1063/1.4981190

[7] Owens B. N. (2019). *The wind power story: A century of innovation that reshaped the global energy landscape*. John Wiley & Sons. https://doi.org/10.1002/9781118794289

[8] Tong W. (2010). *Wind power generation and wind turbine design*. WIT press.

[9] Letcher T. (Ed.). (2023). *Wind energy engineering: A handbook for onshore and offshore wind turbines*. Elsevier. https://doi.org/10.1016/B978-0-323-99353-1.00025-6

[10] Zhou T., & Rempfer, D. (2013) Numerical study of detailed flow field and performance of Savonius wind turbines, *Renewable Energy*, *51*, 373-381. https://doi.org/10.1016/j.renene.2012.09.046

[11] Didane D. H., Bajuri, M. N. A., Manshoor, B., & Boukhari, M. I. (2022) Performance investigation of vertical axis wind turbine with savonius rotor using computational fluid dynamics (CFD), *CFD Letters*, *14(8)*, 116-124. https://doi.org/10.37934/cfdl.14.8.116124

[12] Al-Ghriybah M., Zulkafli, M. F., Didane, D. H., & Mohd, S. (2020) Performance of the savonius wind rotor with two inner blades at low tip speed ratio. *CFD Letters*, *12(3)*, 11-21. https://doi.org/10.37934/cfdl.12.3.1121

[13] Ferrari G., Federici, D., Schito, P., Inzoli, F., & Mereu, R. (2017), CFD study of Savonius wind turbine: 3D model validation and parametric analysis, *Renewable Energy*, *105*, 722-734. https://doi.org/10.1016/j.renene.2016.12.077

[14] Laws P. (2022). Validating the ideal configuration and mutual coupling effect among Savonius wind turbine clusters using free rotation analysis. *Ocean Engineering*, *266*, 112879. https://doi.org/10.1016/j.oceaneng.2022.112879

[15] Didane, D. H., Kudam, D. A., Zulkafli, M. F., Mohd, S., Batcha, M. F. M., & Khalid, A. (2021). Development and performance investigation of a unique dual-rotor Savonius-type counter-rotating wind turbine. International Journal of Integrated Engineering, 13(6), 89-98. https://doi.org/10.30880/ijie.2021.13.06.008

[16] Kim Y., Kumar, S. K. S., Park, Y., Kwon, H., & Kim, C. G. (2020). High-velocity impact onto a high-frictional fabric treated with adhesive spray coating and shear thickening fluid impregnation, *Composites Part B: Engineering*, *185*, 107742. https://doi.org/10.1016/j.compositesb.2020.107742

[17] Wenehenubun F., Saputra, A., & Sutanto, H. (2015). An experimental study on the performance of Savonius wind turbines related with the number of blades, *Energy Procedia*, *68*, 297-304. https://doi.org/10.1016/j.egypro.2015.03.259

[18] Sudarma A. F., Kholil, M., Subekti, S., & Almahdy, I. (2020) The effect of blade number on small horizontal axis wind turbine (HAWT) performance: An experimental and numerical study, *International Journal of Environmental Science and Development*, *11(12).* https://doi.org/10.18178/ijesd.2020.11.12.1307

[19] Kong F., Wu, T., & Hu, J. (2009, September). Study of swept and curved blade influences on HAWT performance. In *2009 World Non-Grid-Connected Wind Power and Energy Conference* (pp. 1-5). IEEE. https://doi.org/10.1109/WNWEC.2009.5335819

[20] Savonius S. J. (1931). The S-rotor and its applications. *Mechanical Engineering*, *53*(5).

[21] Zhiqiang L., Yunke, W., Jie, H., Zhihong, Z., & Wenqi, C. (2018) The study on performance and aerodynamics of micro counter-rotating HAWT, *Energy*, *161*, 939-954. https://doi.org/10.1016/j.energy.2018.07.049

[22] Didane D. H., Behery, M. R., Al-Ghriybah, M., & Manshoor, B. (2024), Recent progress in design and performance analysis of vertical-axis wind turbines—A comprehensive review. *Processes*, *12*(6), 1094. https://doi.org/10.3390/pr12061094

[23] Iswahyudi S., & Wibowo, S. B. (2020). Effect of blade tip shapes on the performance of a small HAWT: An investigation in a wind tunnel, *Case Studies in Thermal Engineering*, *19*, 100634. https://doi.org/10.1016/j.csite.2020.100634

[24] Kumar R. S., Premkumar, T. M., Seralathan, S., Xavier, D. D., Elumalai, E. S., Hariram, V., & Sabapathi, S. (2020). Simulation studies on influence of shape and number of blades on the performance of vertical axis wind turbine. Materials Today: Proceedings, 33, 3616-3620. https://doi.org/10.1016/j.matpr.2020.05.665